Review paper

Cite as: Pandya S, Melville DM: Evaluation of the knee joint with ultrasound and magnetic resonance imaging. J Ultrason 2023; 23: e239–e250. doi: 10.15557/JoU.2023.0032.

Submitted: 04.07.2023
Accepted: 21.07.2023
Published: 30.10.2023

Evaluation of the knee joint with ultrasound and magnetic resonance imaging

Siddharth Pandya[1], David M. Melville[2]

[1] *Department of Radiology, Valleywise Health Medical Center, Phoenix, USA*
[2] *Department of Radiology, Mayo Clinic Arizona, Phoenix, USA*

Corresponding author: David M. Melville; e-mail: melville.david@mayo.edu

DOI: 10.15557/JoU.2023.0032

Keywords
ultrasound; knee; meniscus; ligaments; MRI

Abstract

The knee joint relies on a combination of deep and superficial structures for stability and function. Both ultrasound and high-resolution magnetic resonance imaging are extremely useful in evaluating these structures and associated pathology. This article reviews a combination of critical anatomic structures, joint abnormalities, and pathologic conditions at the knee joint, while highlighting the merits, limitations, and pitfalls of the two imaging modalities. A clear appreciation of each method paired with its relative strengths will aid in expediting diagnosis and appropriate treatment for a wide range of knee joint conditions.

Introduction

The knee is a complex and commonly injured joint with a combination of deep and superficial structures, including cartilage, menisci, ligaments, and tendons, which can be affected by a wide range of pathologic conditions. The primary advanced modality for evaluating knee joint conditions is magnetic resonance imaging (MRI), given its high tissue contrast and ease of diagnosing intra-articular pathology[1]. However, MRI can be quite costly, and some patients are unable to undergo MRI examinations due to certain implanted devices. Ultrasound (US) is a cost-effective alternative that can be performed in point-of-care settings to evaluate many superficial and some internal structures of the knee[2]. In addition, US is often the preferred imaging modality for therapeutic interventions and dynamic imaging of the knee[3]. However, despite its wide availability, US can be operator-dependent and has limited utility for evaluating deeper structures and certain cartilage compartments[4]. This article describes the merits and limitations of both MRI and US in evaluating common knee pathology.

Joint effusion and synovitis

Fluid distention of the knee joint recesses by an effusion is a key marker of underlying joint pathology, including trauma, degeneration, inflammation, or infection. Both US and MRI permit detection of small amounts of fluid not readily apparent on physical examination and radiographs[5,6]. Identification of synovial hypertrophy further aids in the diagnosis of inflammatory and proliferative conditions, including pigmented villonodular synovitis and synovial chondromatosis[7].

Routine non-contrast enhanced knee MRI provides a complete assessment of the various knee joint recesses, including the suprapatellar recess, the lateral and medial joint recesses deep to the patellar retinacula, and the subpopliteus recess[8]. To ensure comprehensive examination for joint fluid with US, all joint recesses should be evaluated to identify small amounts of fluid and account for differences in fluid distribution due to positioning[7]. With the knee in a slightly flexed position, fluid is normally seen in the suprapatellar recess deep to the quadriceps tendon and superficial to the prefemoral fat pad; however, with full knee extension, small amounts of fluid may only be visible in the medial and lateral recesses[9]. At US simple knee joint fluid is anechoic, while the presence of infection, hemorrhage, or crystal-deposition potentially creates a complex appearance. With MRI, an uncomplicated knee joint effusion follows typical fluid signal characteristics, high on fluid-sensitive and intermediate on T1-weighted images.

Both US and MRI offer superior evaluation of joint fluid characteristics compared to radiographs[5]. At US, hemarthrosis results in hyperechoic fluid, and MRI depicts layering blood products or hemosiderin deposition, depending on chronicity. Both modalities accurately diagnose lipohemarthrosis by detecting the presence of a fat-fluid level with greater sensitivity compared to radiographs (Fig. 1)[10,11]. While US potentially visualizes underlying superficial fractures involving the patella, femur, and tibial plateau, MRI permits a complete assessment of intra-articular etiologies in the setting of lipohemarthrosis, including cruciate ligament tear. Fluid complexity is readily evaluated with dynamic maneuvers to demonstrate compressibility and swirling of debris, which helps differentiate a complex, heterogeneously hypoechoic effusion from synovitis[2].

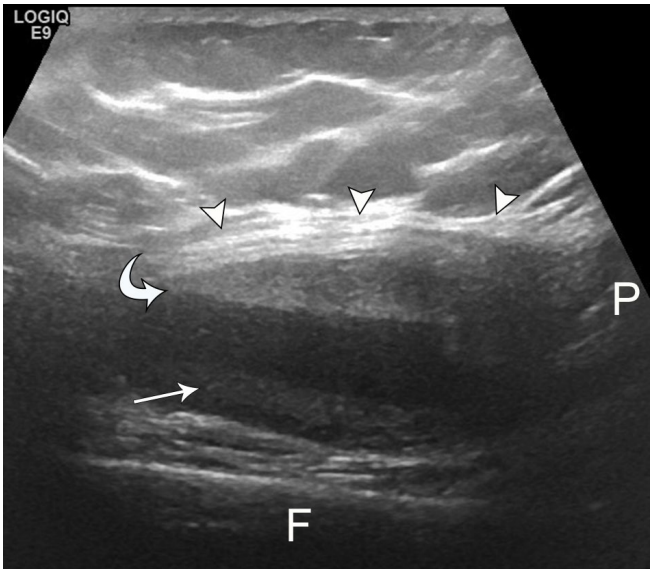

Fig. 1. *62-year-old female with minimally displaced tibial plateau fracture and lipohemarthrosis. Longitudinal grayscale US image superior to the patella demonstrates non-dependent echogenic material (curved arrow) deep to patellar tendon (arrowheads) and subtle layering heterogeneous debris (arrow), representing fat and hemorrhage, respectively, with distinct fat-fluid level in a large joint effusion. P – patella, F – femur*

Doppler US allows identification of active synovitis, which demonstrates increased vascularity associated with hypoechoic, noncompressible synovial thickening (Fig. 2). MRI assessment of synovitis typically relies on intravenous gadolinium contrast to identify thickened or irregular enhancing synovium[12]. In the absence of contrast, hypointense T1-weighted and hyperintense PD/T2-weighted signals serve as surrogate markers, but poorly distinguish synovitis from effusion[1]. Due to rising concerns about gadolinium-based contrast agents, researchers have begun investigating alternative non-contrast sequences for the evaluation of synovitis, including various inversion recovery sequences and a hybrid quantitative double-echo in steady-state (qDESS) technique, with increasing promise[12,13].

Similarly, emerging research with contrast-enhanced US (CEUS) demonstrates greater sensitivity for detecting synovitis related to osteoarthritis compared to power Doppler and contrast-enhanced MRI[14].

Unlike MRI, US allows for both assessment and sampling of joint fluid, when present. Further, US permits the targeting of small volume focal fluid, unlike fluoroscopy[15]. Additionally, US offers the benefit of identifying potentially infected superficial collections to be avoided, which will not be visible during fluoroscopic aspirations. If necessary, US also effectively guides therapeutic joint injections and synovial biopsies. When performing aspirations, it is again important to assess the medial and lateral recesses due to preferential accumulation in the supine position with knee extension.

While effusions can be quickly evaluated and aspirated with US, there is often difficulty in distinguishing infected versus sterile effusions by imaging, as both may demonstrate synovial thickening and hyperemia, particularly in the setting of joint degeneration, inflammatory and metabolic arthropathies, or recent surgery[2]. Even though joint aspiration remains the primary approach to establishing the diagnosis, MRI offers added utility when the diagnosis cannot be readily established by aspiration or when complications are suspected, such

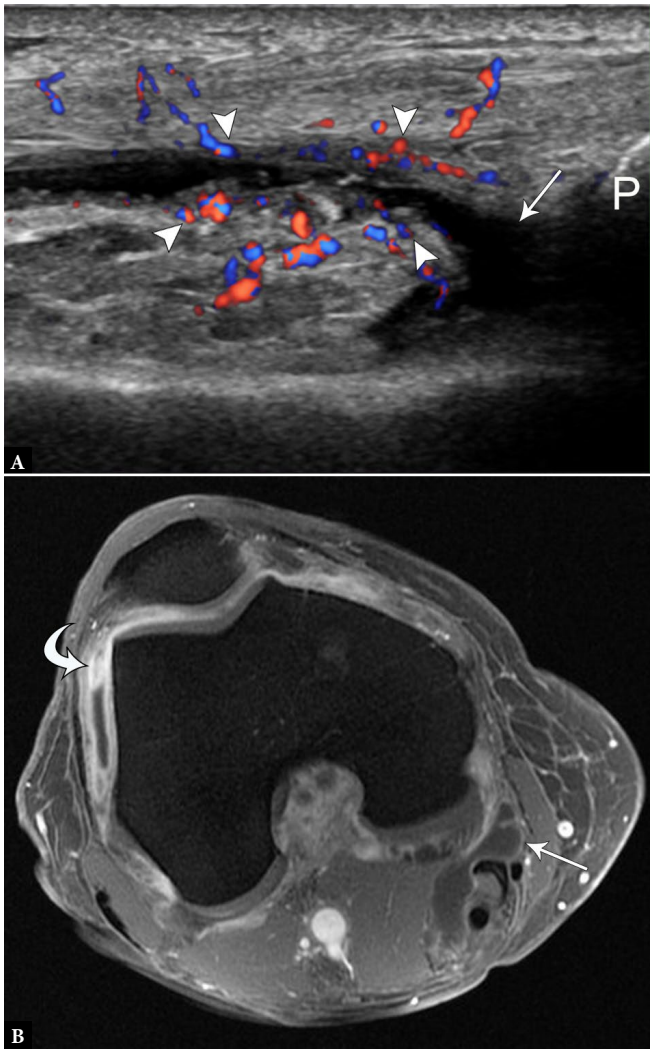

Fig. 2. *57-year-old female with osteoarthritis and synovitis.* **A.** *Longitudinal color Doppler US image superior to the patella (P) demonstrates small suprapatellar joint effusion (arrow) with hyperemic, thickened peripheral synovium (arrowheads).* **B.** *Post-contrast axial spoiled gradient echo MR image of the knee shows thickened and enhancing synovium, most prominent in the lateral gutter (curved arrow), compared to normal synovial enhancement of a Baker's cyst (arrow). P – patella*

as concomitant osteomyelitis and intra-osseous abscess[6]. While both MRI and US may demonstrate erosions, MRI provides a more detailed assessment for the presence and extent of articular cartilage destruction in the setting of aggressive infection[6,16].

Gout

With prevalence increasing alongside rising rates of obesity, gout is now the most common cause of inflammatory arthritis in men and post-menopausal women[17]. The knee is the second most common site of gout involvement, frequently complicated by a wide range of presentations and differential considerations[18].

US allows the detection of intra-articular monosodium urate crystals, and one of the most specific diagnostic findings, the double contour sign, is a hyperechoic layer overlying the superficial margin

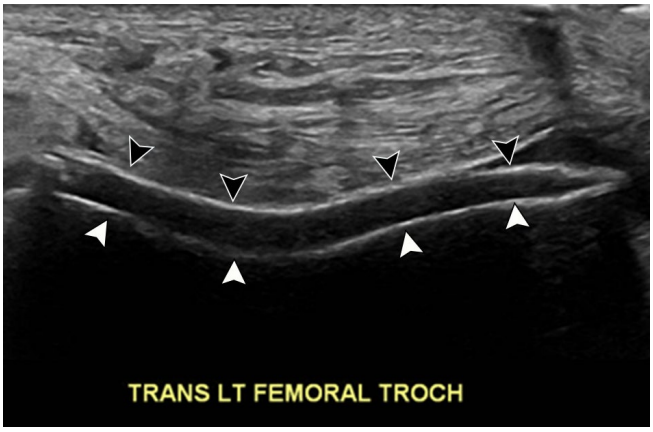

Fig. 3. *76-year-old male with acute-onset left knee pain and history of gout. Transverse grayscale US image at the level of the femoral trochlea demonstrates smooth hyperechoic layer (black arrowheads) overlying the hypoechoic hyaline articular cartilage and paralleling the hyperechoic subchondral bone (white arrowheads), consistent with layering uric acid crystals*

of the anechoic hyaline articular cartilage atop the hyperechoic subchondral bone (Fig. 3)[19]. This sign may be readily visualized at the distal femoral trochlear cartilage by maximally flexing the knee and placing the transducer superior to the patella. With a reported sensitivity and specificity up to 43.7% and 99%, respectively, this finding disappears when the serum uric acid level decreases below 6 mL/dL[7,20]. As a result, it is best relied upon for diagnosing acute gout episodes and monitoring treatment response. It is important not to mistake the hyperechoic foci within the hyaline articular cartilage seen with calcium pyrophosphate deposition for gout[21].

One of the most common superficial sites of tophus deposition is the patellar tendon[7]. At this location, deposits expand and infiltrate, resulting in a pseudotumor appearance; thus, familiarity with the MRI and US appearances of tophus avoids unnecessary biopsy or additional intervention (Fig. 4)[18]. At US, tophi appear as cloud-like hyperechoic nodular or infiltrative foci with a surrounding hypoechoic rim[7]. Posterior acoustic shadowing may be present along with punctate internal foci suggesting the presence of associated calcification, often related to impaired calcium metabolism[20]. Tophi on MRI tend to demonstrate intermediate to low signal intensity on T1-weighted images with heterogeneous T2-weighted signal intensity[18,22]. Other common superficial sites in the knee include the distal quadriceps and proximal popliteus tendons[2].

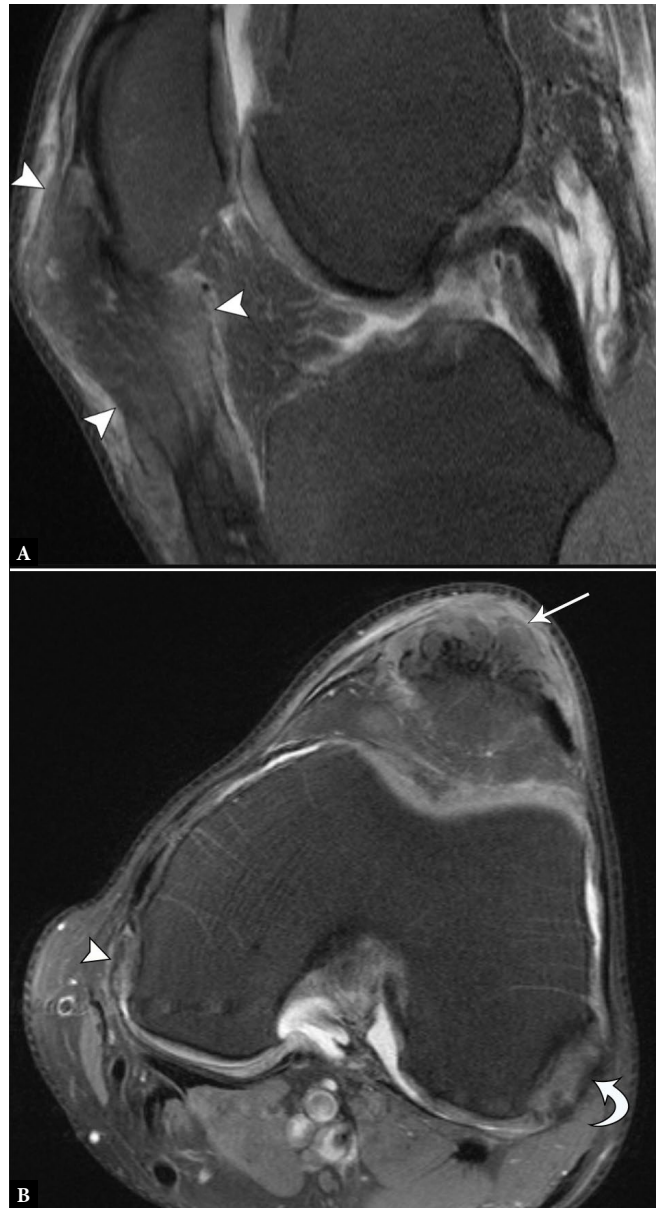

Fig. 4. *39-year-old male with tophaceous gout presenting as a palpable peripatellar mass.* ***A.*** *Sagittal proton-density-weighted fat-suppressed MR image shows expansile intermediate-signal soft tissue (arrowheads) within the patellar tendon, extending superficial to the anterior patella.* **B.** *Axial proton-density-weighted fat-suppressed image shows the mass in the patellar tendon (arrow), as well as additional heterogeneously intermediate-signal nodules within the popliteus tendon (curved arrow) and along the medial femoral condyle (arrowhead), in a distribution characteristic of tophaceous gout*

Cruciate ligament tears

With their deep position, visualizing the entirety of the cruciate ligaments at US is challenging[23]. To evaluate the cruciate ligaments at US, the patient is placed prone, with the knee flexed at approximately 20 degrees[24]. The tibial insertion of the anterior cruciate ligament (ACL) may be better visualized with the patient in the supine position, with maximal passive flexion of the knee (Fig. 5 A)[25]. The probe is oriented longitudinally along the patellar tendon with rotation of the cranial aspect of the probe towards the medial aspect of the lateral femoral condyle[26]. Patient pain and swelling potentially limit visibility with this approach.

Even with optimal positioning, the ACL remains difficult to directly visualize, and diagnosis of tear relies on indirect signs, such as abnormal hypoechogenicity or a discrete fluid collection in the expected location of the ACL[23]. The tibial insertion of the posterior cruciate ligament (PCL) is directly visible when imaging with the posterior approach (Fig. 5 B)[2]. Heterogeneity and/or thickening of the PCL >10 mm with ill-defined margins at US reflects injury, but does not readily identify proximal tears (Fig. 6)[27].

Fig. 5. *53-year-old female with knee pain, unable to undergo MRI.* **A.** *Longitudinal grayscale US image slightly oblique to the patellar tendon with knee flexion demonstrates no tear at the tibial insertion of the anterior cruciate ligament (ACL) (arrowheads). T – tibia, F – femur.* **B.** *Longitudinal grayscale US image at the central posterior tibial plateau with knee flexion demonstrates no tear at the tibial insertion of the posterior cruciate ligament (PCL) (arrowheads). The femoral origin of either ligament is not visible*

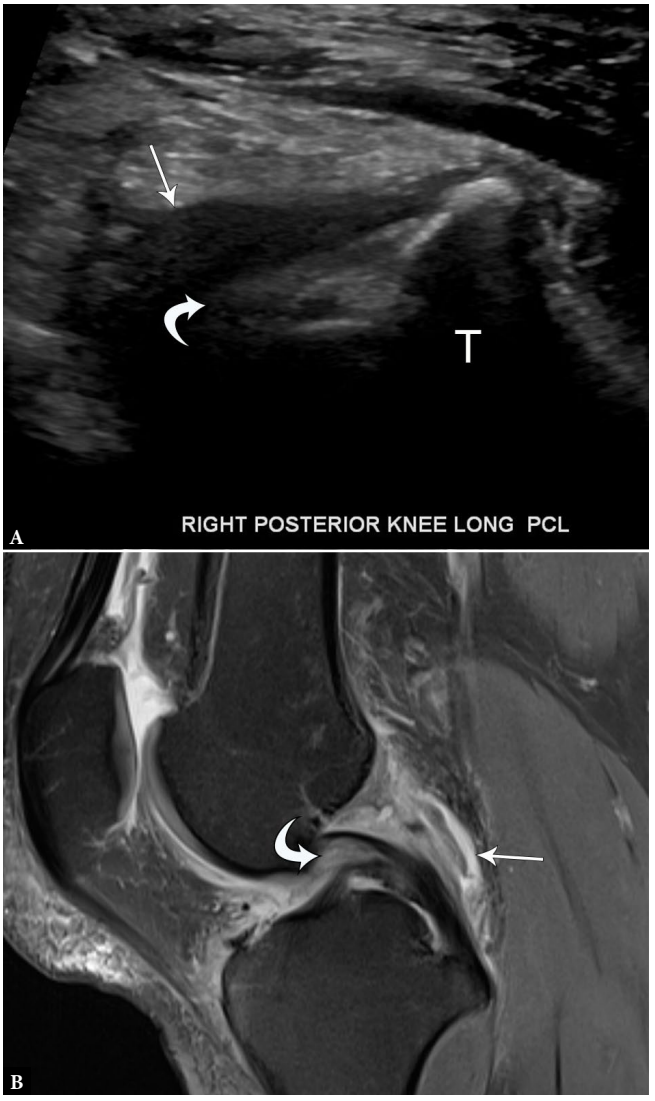

Fig. 6. *33-year-old male with partial posterior cruciate ligament tear.* **A.** *Longitudinal grayscale US image of the PCL demonstrates normal tibial attachment but indistinct, hypoechoic proximal fibers (curved arrow) with surrounding hypoechoic material (arrow).* **B.** *Sagittal proton-density-weighted fat-suppressed MR image shows edema and thickening of the proximal PCL (curved arrow) with surrounding edema and fluid (arrow)*

Due to the limitations of US, MRI remains the primary modality for the evaluation of cruciate ligament tears. In the setting of limited MRI availability, dynamic US with asymmetric anterior tibial translation compared to the contralateral side >3 mm has been identified as a potential screening parameter; however, the reliability is confounded in the presence of chronic tears, prior contralateral injury, or ACL reconstruction involving either side[24]. A retrospective review of dynamic US imaging of ACL tears with arthroscopic correlation revealed a negative predictive value of 95% for complete ACL tears, further supporting US as a point-of-care screening test[26]. While US is useful for superficial graft complications (Fig. 7), MRI allows complete visualization of the graft (Fig. 8).

Collateral ligament tears

While many orthopedic surgeons rely on clinical history and physical examination to diagnose and grade collateral ligament injuries, significant trauma or concern for multi-ligamentous injury prompts imaging evaluation to guide surgical intervention[28]. Unlike the cruciate ligaments, both the medial collateral ligament (MCL) and the lateral collateral ligamentous (LCL) complex are superficially located, allowing a rapid focused US assessment.

The medial collateral ligament (MCL) is composed of three discrete layers, and the key stabilizing component is the middle layer, also referred to as the tibial collateral ligament or superficial MCL (Fig. 9 A)[29].

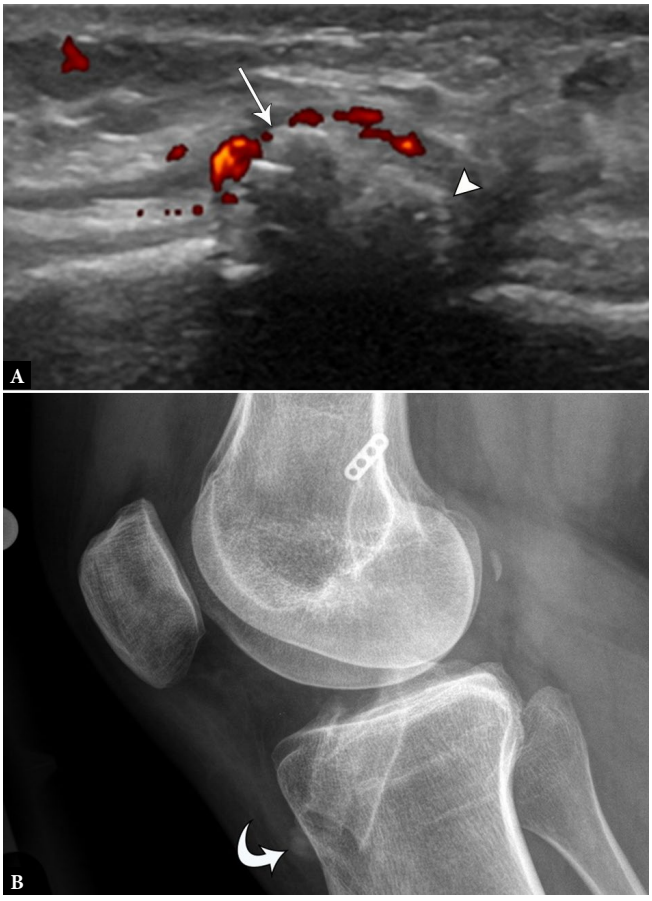

Fig. 7. *25-year-old female with anterior tibial pain and palpable lump following ACL reconstruction.* **A.** *Longitudinal power Doppler US image of the anterior tibial cortex in the area of focal pain identifies a protruding interference screw (arrow) with adjacent hyperemia and reactive bone formation (arrowhead).* **B.** *Follow-up knee radiograph identifies proud interference screw (curved arrow) corresponding to US findings*

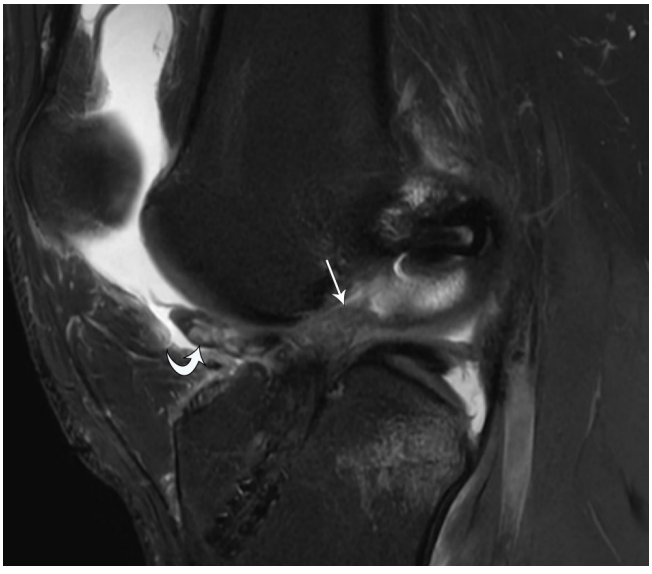

Fig. 8. *20-year-old male with complete ACL graft rupture. Sagittal proton-density-weighted fat-suppressed MR image shows complete disruption of the ACL graft (arrow) with anteriorly displaced torn graft fibers (curved arrow)*

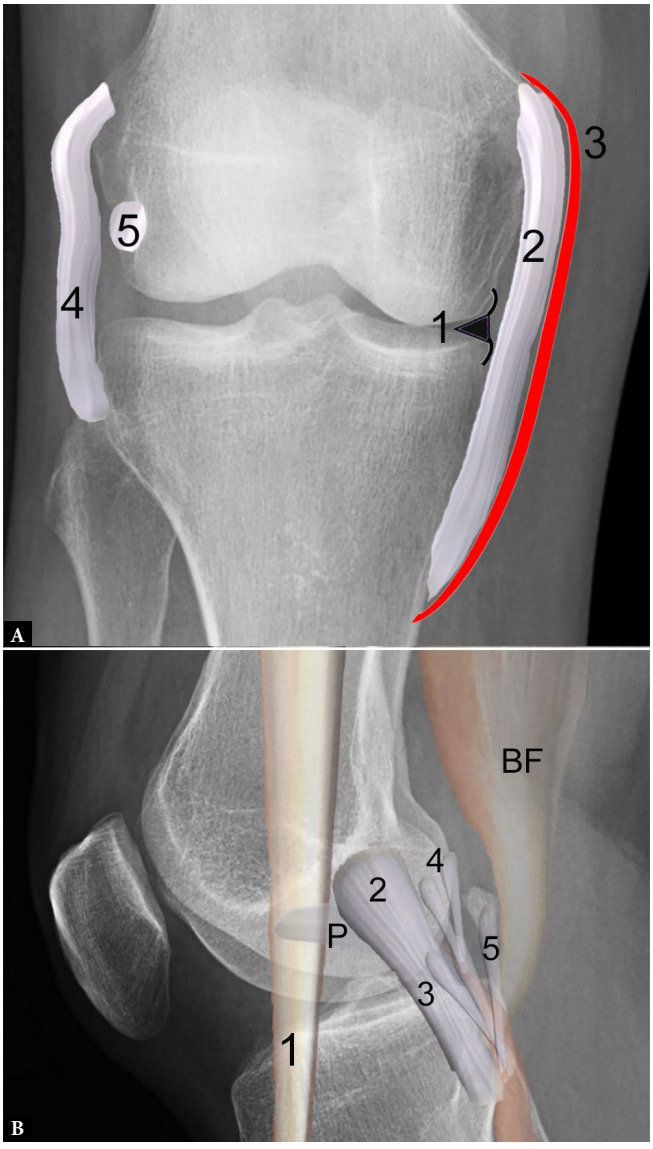

Fig. 9. *Illustrations of medial and lateral supporting structures at the knee joint superimposed on radiographs.* **A.** *Illustration of medial collateral ligament (MCL) complex superimposed on PA view of the knee shows the medial meniscal body (1) with deep layer consisting of the attached meniscofemoral and meniscotibial ligaments, middle layer consisting of the tibial collateral ligament (or superficial MCL) (2), with superficial layer composed of crural fascia (3). Note the fibular collateral ligament (4) and popliteus tendon (5) at the lateral knee.* **B.** *Illustration of lateral supporting structures, including the iliotibial band (1), fibular collateral ligament (2) running from the femoral condyle to the fibular head and attaching near the biceps femoris (BF) tendon insertion, as well as the posterolateral corner structures consisting of the popliteofibular ligament (3) arising from the fibular styloid and attaching to the popliteus (P) myotendinous junction, the Y-shaped arcuate ligament (4), and the fabellofibular ligament (5)*

The superficial MCL is the most commonly injured knee ligament, easily identified on US by positioning the probe in the true coronal plane along the medial joint line, with minor adjustments in the anterior and medial directions until its linear fibrillar appearance is brought into a long-axis view[28]. Turning the probe perpendicularly allows visualization of the short axis, which is evaluated from the medial femoral condyle to the tibial insertion[28]. As the probe is moved

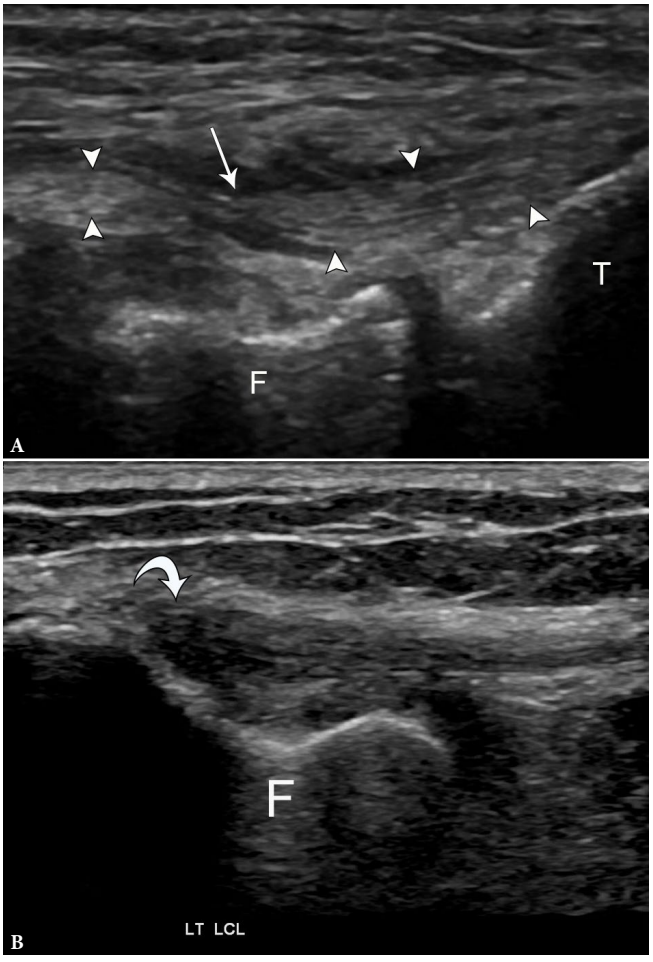

Fig. 10. *75-year-old female with high-grade partial fibular collateral ligament (FCL) injury.* **A.** *Longitudinal grayscale US image along the course of the FCL (arrowheads) next to the femoral popliteal groove (F) and tibial plateau (T) demonstrates attenuated remnant fibers with surrounding fluid (arrow). Compare to the normal appearance of the FCL on longitudinal grayscale US image* **B.** *with anisotropy (curved arrow) at the proximal portion*

distally, the pes anserinus tendons are noted superficial to the MCL as they course toward their distal insertions on the anteromedial tibia. The normal ligament appears hyperechoic, with a compact fibrillar architecture, extending from the medial femoral condyle to the proximal tibia approximately 6 cm distal to the joint line[7].

The lateral collateral ligamentous complex consists of lateral and posterolateral corner supporting structures. The primary restraint to varus stress is the fibular collateral ligament (FCL), the US probe is placed in the coronal plane along the lateral joint line until the popliteal groove of the lateral femoral condyle is identified. The proximal aspect of the transducer is fixed on the groove as the distal portion is rotated posteriorly until the fibular head enters the field of view. In this position, the typical fibrillar appearance of the FCL should be visible. To avoid fiber undulation and resultant anisotropy, which may mimic injury, valgus angulation of the knee should be avoided during this assessment[2].

Additional lateral supporting structures include the popliteus muscle and tendon, biceps femoris tendon, as well as the popliteofibular, arcuate and fabellofibular ligaments (Fig. 9 B). Along with the joint capsule and lateral patellar retinaculum, the lateral gastrocnemius tendon and iliotibial tract provide additional lateral stabilization. MRI allows for a rapid comprehensive assessment of these numerous structures, particularly in the setting of acute multiligamentous injury[30].

At US, collateral ligament injuries range from hypoechoic ligamentous thickening, partial fiber disruption, or a full-thickness tear with interposed fluid and heterogeneous debris (Fig. 10). In the setting of distal MCL tears, it is important to assess the relationship of the torn ligamentous fibers and the overlying pes anserinus to identify a Stener-like MCL tear. With this injury, the torn and displaced MCL fibers are superficial to the pes anserine tendons, preventing adequate healing and necessitating surgical repair to restore stability (Fig. 11)[31]. For partial-thickness or non-displaced complete tears, shear wave

Fig. 11. A. *19-year-old male with displaced MCL tear. Coronal proton-density-weighted fat-suppressed MR image shows completely torn and proximally displaced MCL stump (curved arrow) superficial to the pes anserinus, consistent with a Stener-like lesion.* **B.** *16-year-old male with flipped and entrapped MCL tear. Coronal proton-density-weighted fat-suppressed MR image shows completely torn and proximally displaced MCL stump entrapped at the medial joint line inferior to the meniscus (arrow), which also requires surgical repair despite lying deep to the pes anserinus.*

elastography and power Doppler imaging may prove useful to assess collateral ligament healing, particularly in high-performance athletes[32,33]. Laxity of an injured ligament is associated with decreasing shear wave velocities, or "softening" of the ligament, and may be associated with a functional decline[32]. A biomechanical elastography study identified the greatest relative stiffness of the MCL during full knee extension and suggested that return to play could be determined by loading the injured collateral ligament at progressively lower flexion angles, while assessing for gradually improving ligament stiffness[34]. Comparison to the stiffness of the uninjured contralateral side provides a valuable reference range. Ongoing studies continue to explore the clinical significance of elastography in monitoring recovery and risk of recurrent injury in athletes.

A recent systematic review identified MRI as the most common imaging method for evaluating collateral ligament injuries[35], and MRI is considered the imaging gold standard[28]. According to this review, MRI fared well in grading injury severity, but detected the location of injury less reliably, particularly with obliquely oriented MCL ruptures[35]. Another recent study noted only a "fair" agreement between MRI and the clinical grade, with MRI frequently overestimating the injury grade[36]. Despite these shortcomings, there was a notable degree of consensus with respect to the diagnosis and localization of the surgically-significant Stener-like lesions[37].

On MRI, the ligaments are hypointense structures and pathology is visualized as intrasubstance hyperintense edema and fluid on fluid-sensitive sequences. If concerned about isolated collateral ligament injuries, US functions well for focused examinations, with a diagnostic accuracy for MCL injuries of up to 94%[38].

In the absence of complete MCL tears or concomitant ligamentous injuries, static MR images provide limited information regarding joint stability[35,36]. Dynamic imaging with US during applied stress provides an alternative to conventional stress radiographs and fluoroscopy[39]. To evaluate MCL instability, the knee is placed in a neutral position, with the probe oriented longitudinally in the coronal plane at medial joint line; valgus stress is then applied to the knee, and the amount of medial joint space widening is measured. Multiple studies have shown that joint space widening of less than 5 mm corresponds to grade 1 injury, while widening of 5–10 mm corresponds to grade 2 injury, and widening over 10 mm corresponds to grade 3 injury[38]. A similar technique can be used for the LCL complex and lateral joint space widening of >10.5 mm with varus stress serves as an indirect sign for a posterolateral corner injury[40].

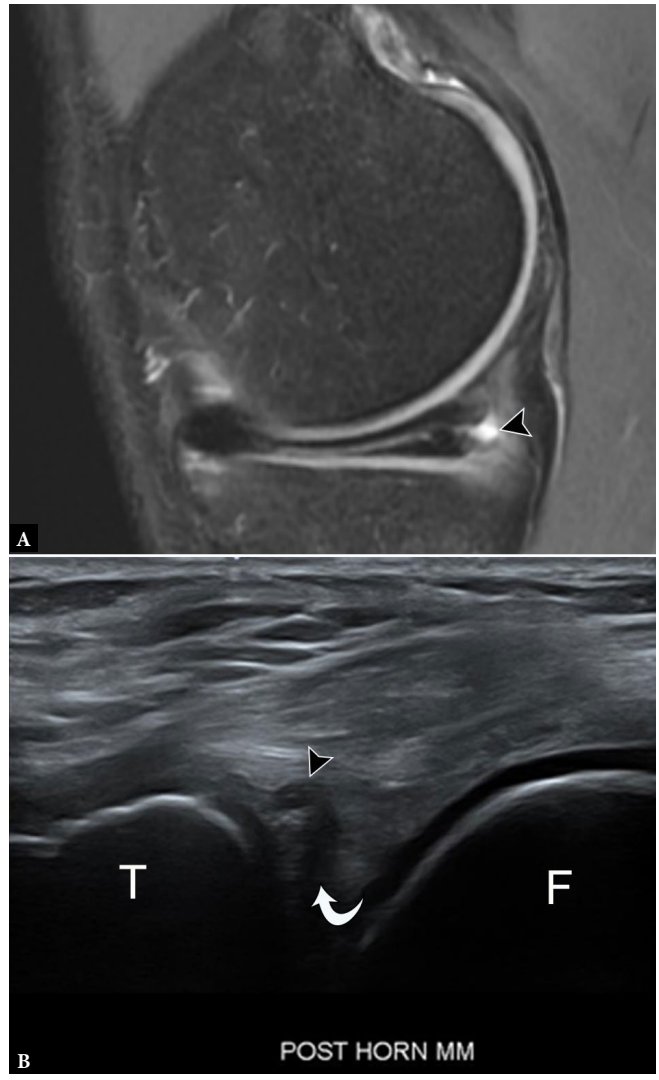

Fig. 12. *37-year-old male with horizontal meniscal tear and small parameniscal cyst.* **A.** *Sagittal proton-density-weighted fat-suppressed MR image demonstrates horizontal tear extending from the free edge of the medial meniscus to the periphery, with associated parameniscal cyst (arrowhead).* **B.** *Longitudinal grayscale US image of the posterior knee shows a horizontally oriented, hypoechoic cleft, consistent with a tear (curved arrow), in the echogenic, triangular posterior meniscus with a small, contiguous parameniscal cyst (arrowhead). T – tibia, F – femur*

Meniscal pathology

MRI is regarded as the imaging gold standard for meniscal evaluation, and US is not reliable as a sole imaging modality[2,4]. A meta-analysis of 27 studies reveals MRI sensitivity and specificity of 93% and 88% for medial meniscal tears, and 79% and 96% for lateral meniscal tears, respectively[41]. On both T1-weighted and T2-weighted imaging, the normal fibrocartilaginous menisci are hypointense triangular structures. Meniscal degeneration is defined as increased linear or globular intrasubstance fluid-signal not disrupting a meniscal surface[42]. Fluid-signal intensity extending to the meniscal articular surfaces on two contiguous slices is diagnostic of a tear (Fig. 12 A). Additionally, MRI can characterize the different types of meniscal tears and the presence or absence of displaced meniscal tissue, which is vital to the orthopedic surgeon in determining surgical versus non-surgical treatment.

On US, only the peripheral portions of the menisci are visualized as triangular hyperechoic structures. Meniscal degeneration is typically visualized as tissue heterogeneity, either with or without extrusion or fragmentation, while a true meniscal tear will appear as hypo- or anechoic linear defects extending to the periphery of the meniscus (Fig. 12 B)[2]. Tears deep to the visible meniscal periphery are difficult to visualize, with a reported sensitivity for medial and lateral meniscal tear as low as 0% and 8%, respectively[4]. While the overall sensitivity and specificity of detecting all meniscal tears on US is 85% and 86%, respectively, US is highly accurate at diagnosing parameniscal cysts, which is a secondary sign of an underlying meniscal tear[2,43].

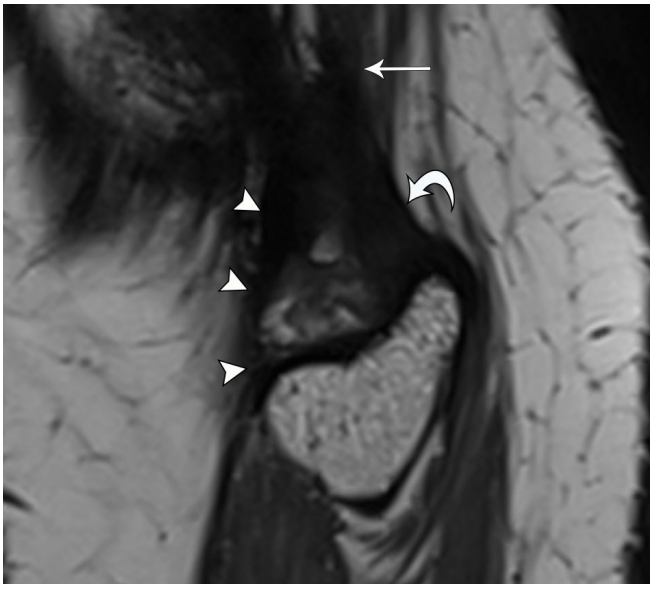

Fig. 13. *33-year-old female with snapping sensation at the lateral knee. Dynamic US imaging (see* Video 1*) shows snapping of the tibial arm of the biceps femoris tendon. Note initial orientation of the probe in the longitudinal plane before turning to short axis before imaging about the fibular head. Sagittal PD SPACE MR image shows thickened tibial arm (arrowheads) bifurcating from the biceps femoris tendon (arrow) and coursing anterior to the fibular arm (curved arrow)*

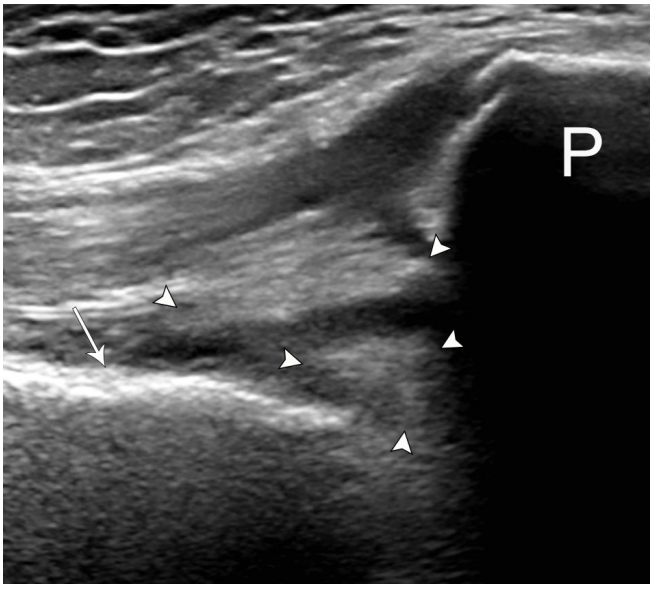

Fig. 14. *63-year-old female with patellar clunk syndrome. Longitudinal grayscale US image shows ovoid and nodular echogenic foci (arrowheads) closely associated with the patella and quadriceps fat pad, located between the superficial quadriceps tendon and echogenic distal femoral arthroplasty hardware (arrow). Technical limitations prevented visualization of nodule motion, but dynamic evaluation elicited discomfort and characteristic clunk*

Snapping knee

A sudden displacement of anatomic structures during knee joint motion results in a snapping sensation. Recurrent snapping potentially leads to pain, discomfort, and limitation of activities. Sources of snapping include extra-articular structures, like the popliteus tendon, pes anserinus, and iliotibial band[3]. Intra-articular etiologies include menisci, plicae, tumors, and joint bodies[44]. One of the most common sources of extra-articular knee snapping is the distal long head biceps femoris tendon[45]. The snap occurs during knee extension, and clinical examination shows abrupt translocation of the biceps tendon over the fibular head[46]. Dynamic real-time visualization of the tendon with US confirms the snapping source during range-of-motion movements. Once the source of snapping is identified, MRI can serve as a useful adjunct for the assessment of anatomy prior to surgical intervention, in particular the evaluation of the direct (fibular) and anterior (tibial) arms of the distal biceps femoris tendon (Fig. 13, Video 1)[47]. Other associations include congenital absence of the direct arm, fibular head hypertrophy, and too-distal bifurcation of the two arms[45].

Snapping also occurs in the post-arthroplasty setting, most frequently resulting from patellar clunk syndrome[45]. Within months or a few years post-arthroplasty, affected patients notice a painful catching sensation or audible snap in the suprapatellar region during knee extension. The condition results from impingement of a suprapatellar fibrous nodule against the intercondylar notch of the femoral prosthesis[48]. The presence of metallic artifact on MRI limits visibility of this fibrotic nodule. On US, the abnormal tissue is typically identified as a hyperechoic nodule at the junction between the superior patellar pole and quadriceps tendon, with visible motion as the knee is extended from a flexed position and the nodule displaces from the intercondylar notch (Fig. 14)[49]. Uncommonly, the nodule may be positioned immediately posterior to the patella, limiting its visibility[50].

While dynamic US provides superior evaluation of extra-articular snapping, MRI lends greater utility in identifying deep intra-articular etiologies. Despite being more frequently associated with locking, meniscal tears may result in snapping. If the snapping segment is peripherally located, US may demonstrate meniscal displacement with provocative maneuvers; however, the underlying tear or discoid meniscus may not be visible[3]. As discussed above, MRI most accurately characterizes tear morphology and extent prior to operative repair. The extent of involvement of additional sources of intra-articular snapping such as exostoses, nodular synovitis and tenosynovial giant cell tumors are better evaluated with MRI[45]. In addition to identifying intra-articular bodies leading to snapping, MRI clearly depicts associated cartilage loss.

Extensor mechanism

Tendinosis and tears of the quadriceps and patellar tendons are common sources of anterior knee pain[2,51]. While diagnosis of both tears and tendinosis involving the extensor mechanism hinges upon clinical examination, MRI and US provide imaging confirmation[5,52]. At US, tendinosis appears as focal thickening and hypoechogenicity, while partial tears are identified as focal hypoechoic defects or clefts in the fibrillar tendon architecture. Full-thickness disruption of the tendon fibers indicates complete tear with varying degrees of retraction (Fig. 15). Point-of-care US in the clinic and emergency setting permits rapid confirmation of suspected extensor tendon pathology.

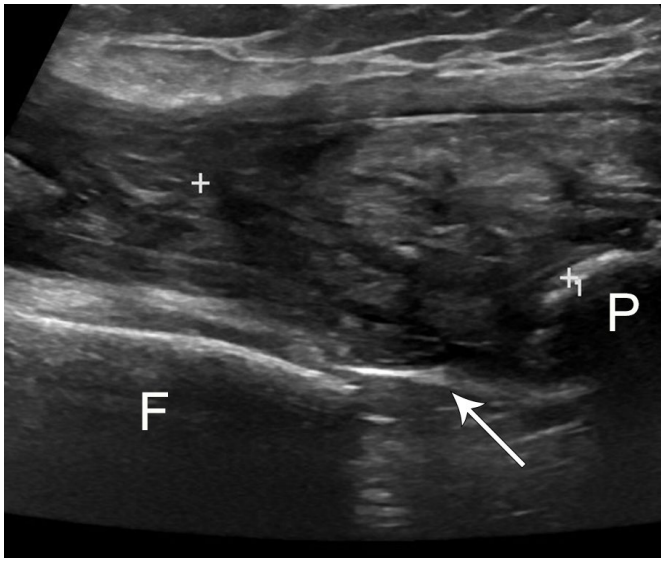

Fig. 15. *74-year-old male with total knee arthroplasty and quadriceps tendon rupture. Longitudinal grayscale US image shows a full-thickness distal quadriceps tendon tear with retraction (between calipers) from the patella insertion with surrounding hematoma. Note brightly echogenic arthroplasty component (arrow) at the distal femur. P – patella, F – femur*

The use of Doppler imaging and elastography increases the sensitivity for the detection of tendinosis with higher tendon stiffness in symptomatic patellar tendinopathy (Fig. 16)[52,53]. Studies demonstrating the evolving elastography properties of the patellar tendon following ACL graft harvesting reveal the future promise in assessing tendon healing in the post-operative and post-traumatic settings[54,55]. This is particularly helpful, as patients may experience symptomatic and functional improvement in the absence of morphological changes on grayscale US, and measurable improvements in tendon stiffness may help predict outcomes and track recovery[56].

Like US, MRI shows thickening and edema with tendinosis and partial or full-thickness fluid-filled defects in the setting of tear. MRI offers the advantage of assessing patellar cartilage defects, particularly in the setting of patellar instability episodes or patellar tracking disorders.

Cysts and cyst-like masses

The knee is a common site to develop cysts and cyst-like masses, as well as other lesions that can mimic cysts[57]. Imaging permits confirmation of a cyst by its appearance, anatomic relationship, and location. Superficial, palpable abnormalities are best assessed initially with US due to its low cost, accessibility, and rapid identification of characteristic imaging features. The typical US appearance of a cyst is a noncompressible anechoic or hypoechoic mass with well-defined, smooth margins. Thin internal septations, lobulations, and posterior acoustic enhancement may also be present.

Popliteal fossa masses are one of the most common indications for knee US, and examination typically reveals a Baker (or popliteal) cyst in the characteristic location between the semimembranosus and medial head of gastrocnemius tendons (Fig. 17 A)[2]. The cyst, actually the combination of the gastrocnemio-semimembranosus and subgastrocnemius bursae, may demonstrate evidence of internal complexity, such as septations, debris, joint bodies, as well as partial or complete rupture with associated tracking fluid and irregular cyst margins (Fig. 17 B)[7]. Other common cystic masses include ganglia, synovial cysts, and parameniscal cysts, as well as additional bursae.

Numerous other synovial-lined anatomical bursae facilitate the movement of muscles and tendons about the knee joint by reducing friction (Fig. 18). Abnormal distention of these bursae may present as masses with varying degrees of associated pain. The anterior knee bursae include the prepatellar bursa along with the superficial and deep infrapatellar bursae[2]. The MCL, pes anserinus, and semimembranosus-tibial collateral ligament bursae are found at the medial

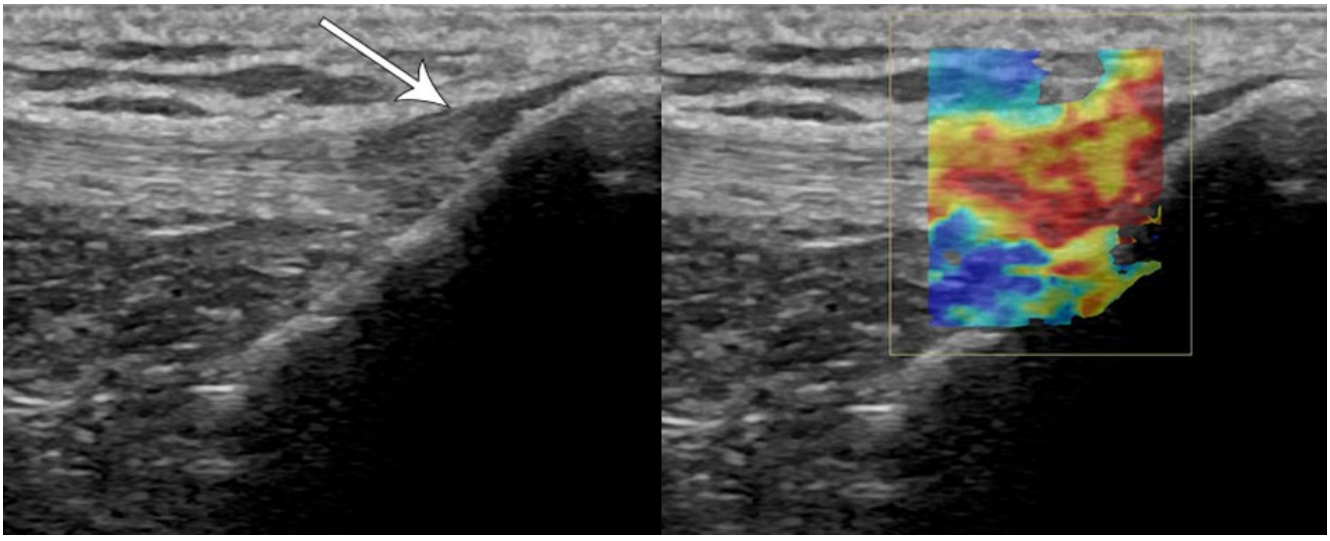

Fig. 16. *65-year-old female with anterior knee pain. Longitudinal grayscale and transient elastography US images of the distal patellar tendon show focal hypoechogenicity and thickening (arrow) with corresponding increased stiffness denoted by overlying color map (increasing stiffness from blue to red), consistent with focal patellar tendinosis*

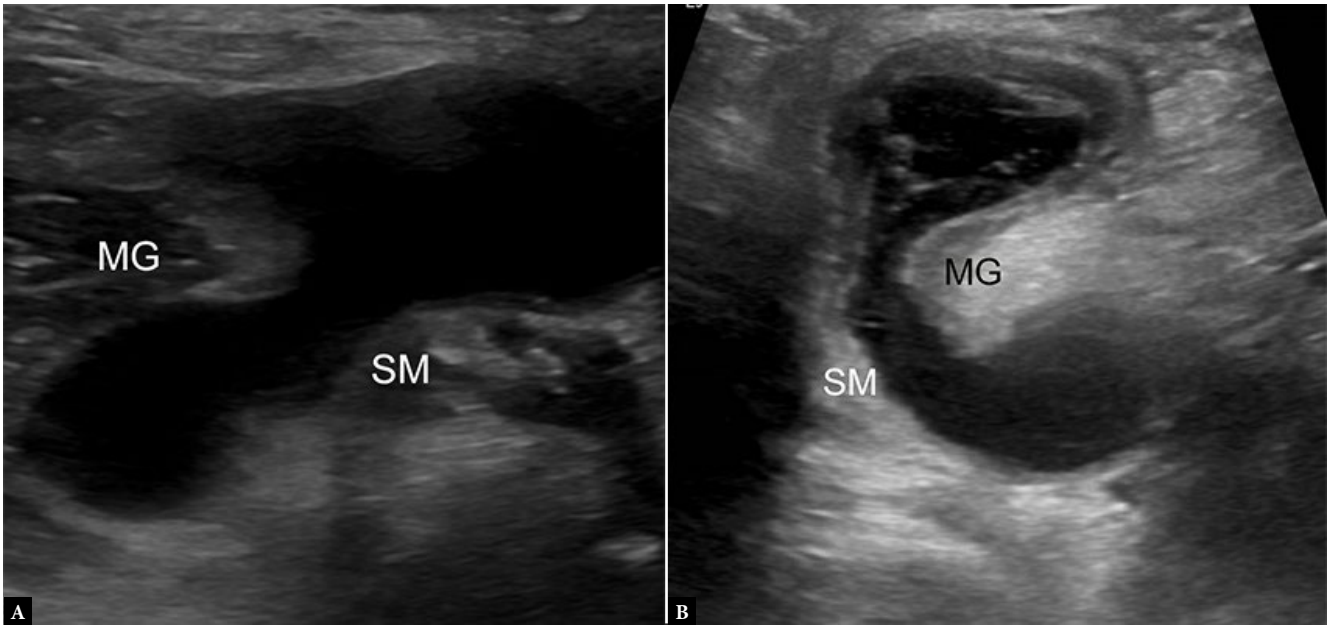

Fig. 17. A. *19-year-old male with Baker's cyst. Transverse grayscale US image of the posterior knee shows bilobed anechoic fluid collection located between the semimembranosus (SM) and medial gastrocnemius (MG) tendons, consistent with a Baker's cyst. Note anisotropy of the SM relative to MG tendon, not to be confused with debris.* **B.** *85-year-old female with complex Baker's cyst. Transverse grayscale US image shows thick-walled collection with internal septations and debris with otherwise typical location and appearance*

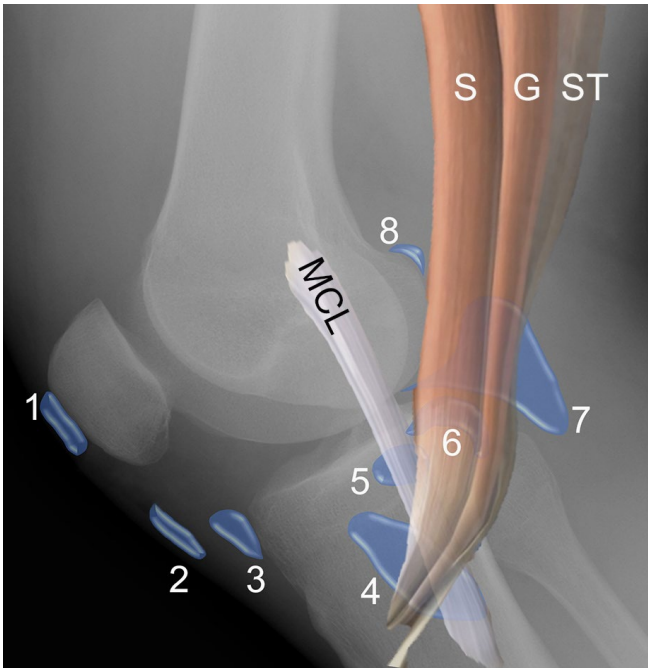

Fig. 18. *Illustration of common bursae located about the knee joint, superimposed on a lateral knee radiograph shows the prepatellar bursa (1), superficial infrapatellar bursa (2), deep infrapatellar bursa (3), pes anserinus bursa (4) deep to the sartorius (S), gracilis (G), and semitendinosus (ST) tendons, MCL bursa (5) deep to the MCL, semimembranosus-tibial collateral ligament bursa (6), Baker cyst (7), medial (8) and lateral (not shown) gastrocnemius bursae*

aspect of the knee. The semimembranosus-tibial collateral ligament bursa is located at the posteromedial aspect of the knee subjacent to the semimembranosus tendon. The characteristic "inverted-U" shape of this bursa help distinguishes it from the nearby pes anserinus bursa, which lies deep to the pes anserinus tendons. Adventitious bursae occur at sites of abnormal pressure and lack a synovial lining. The presence of compressibility allows differentiation of an adventitious bursa from a recurrent tumor in the setting of knee amputation[7]. Though both US and MRI readily diagnose bursal distention, US allows rapid correlation with symptoms, as well as fluid sampling in the setting of potential infection or crystal-deposition disease.

Solid masses identified on US or non-contrast enhanced MRI frequently require further characterization with contrast-enhanced MRI. Any cystic-appearing mass without clear joint contiguity or definite origin on MRI should be viewed with suspicion until a synovial sarcoma is excluded. Popliteal arterial aneurysms and pseudoaneurysms are readily identified by association with the popliteal artery on MRI and US, as well as internal flow at Doppler US (Fig. 19). Any mass that demonstrates deep intra-articular or osseous contiguity will be more completely assessed with MRI.

Conclusion

The complexity of the knee joint predisposes it to many pathologic conditions, all of which can be imaged by MRI and majority by US. While US provides real-time dynamic imaging about the knee and easily evaluates superficial structures, its effectiveness relies upon technical skills, body habitus, and depth of pathology. Conversely, MRI effectively diagnoses abnormalities involving both the superficial and deep structures of the knee; however, it is costly, less widely available, and contraindicated in patients with certain implanted medical devices. It is important for providers to recognize situations when each modality is preferred and their relative limitations in order to maximize the diagnostic potential.

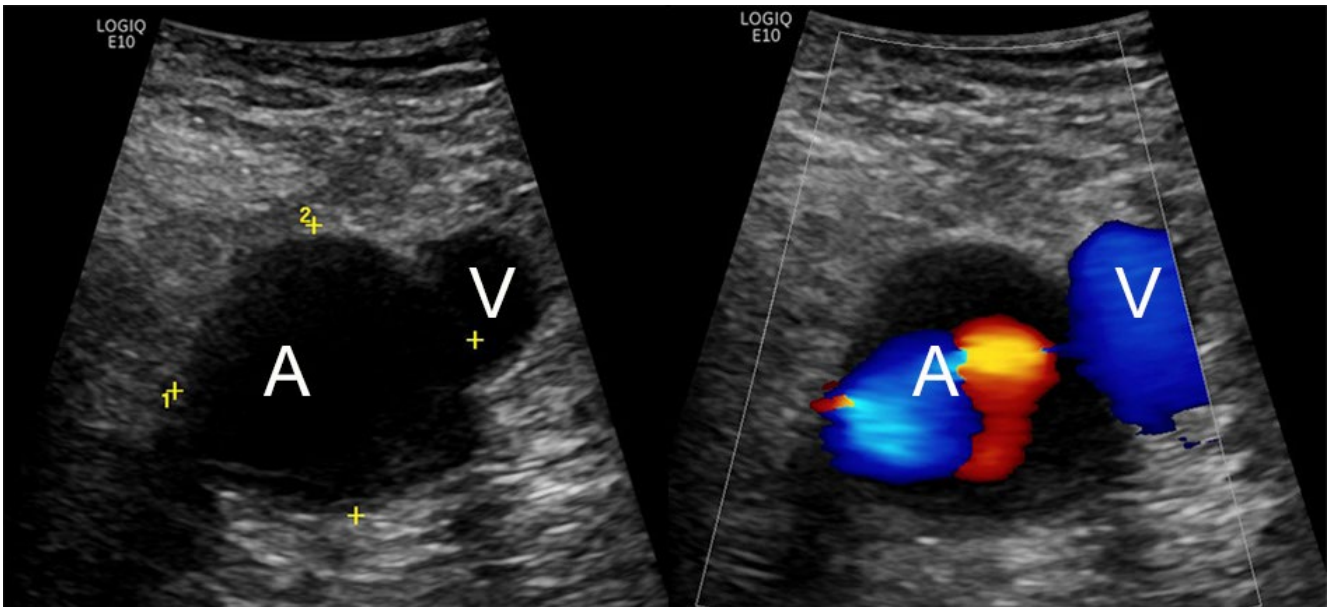

Fig. 19. *69-year-old male with popliteal artery aneurysm. Transverse grayscale and color Doppler US images show enlarged popliteal artery (A) adjacent to the normal vein (V) with internal turbulent flow*

Conflict of interest

The authors do not report any financial or personal connections with other persons or organizations which might negatively affect the contents of this publication and/or claim authorship rights to this publication.

Author contributions

Writing of manuscript: DMM, SP.

References

1. Nacey NC, Geeslin MG, Miller GW, Pierce JL: Magnetic resonance imaging of the knee: An overview and update of conventional and state of the art imaging. J Magn Reson Imaging 2017; 45: 1257–1275. doi: 10.1002/jmri.25620.
2. Alves TI, Girish G, Kalume Brigido M, Jacobson JA: US of the knee: scanning techniques, pitfalls, and pathologic conditions. Radiographics 2016; 36: 1759–1775. doi: 10.1148/rg.2016160019.
3. Khoury V, Cardinal E, Bureau NJ: Musculoskeletal sonography: a dynamic tool for usual and unusual disorders. Am J Roentgenol 2007; 188: W63–73. doi: 10.2214/AJR.06.0579.
4. Bruce W, Lee TS, Sundarajan V, Walker P, Magnussen J, Van der Wall H: Performance characteristics of ultrasound of the knee in a general radiological setting. Knee 2004; 11: 303–306. doi: 10.1016/j.knee.2003.07.006.
5. Basha MAA, Eldib DB, Aly SA, Azmy TM, Mahmoud NEM, Ghandour TM *et al.*: Diagnostic accuracy of ultrasonography in the assessment of anterior knee pain. Insights Imaging 2020; 11: 107. doi: 10.1186/s13244-020-00914-2.
6. Flemming DJ, Hash TW 2nd, Bernard SA, Brian PS: MR imaging assessment of arthritis of the knee. Magn Reson Imaging Clin N Am 2014; 22: 703–724. doi: 10.1016/j.mric.2014.07.012.
7. Jacobson JA, Ruangchaijatuporn T, Khoury V, Magerkurth O: Ultrasound of the knee: common pathology excluding extensor mechanism. Semin Musculoskelet Radiol 2017; 21: 102–112. doi: 10.1055/s-0037-1599204.
8. Fenn S, Datir A, Saifuddin A: Synovial recesses of the knee: MR imaging review of anatomical and pathological features. Skeletal Radiol 2009; 38: 317–328. doi: 10.1007/s00256-008-0570-0.
9. Mandl P, Brossard M, Aegerter P, Backhaus M, Bruyn GA, Chary-Valckenaere I *et al.*: Ultrasound evaluation of fluid in knee recesses at varying degrees of flexion. Arthritis Care Res (Hoboken) 2012; 64: 773–779. doi: 10.1002/acr.21598.
10. Bonnefoy O, Diris B, Moinard M, Aunoble S, Diard F, Hauger O: Acute knee trauma: role of ultrasound. Eur Radiol 2006; 16: 2542–2548. doi: 10.1007/s00330-006-0319-x.
11. Schick C, Mack MG, Marzi I, Vogl TG: Lipohemarthrosis of the knee: MRI as an alternative to the puncture of the knee joint. Eur Radiol 2003; 13: 1185–1187. doi: 10.1007/s00330-002-1375-5.
12. Thoenen J, Stevens KJ, Turmezei TD, Chaudhari A, Watkins LE, McWalter EJ *et al.*: Non-contrast MRI of synovitis in the knee using quantitative DESS. Eur Radiol 2021; 31: 9369–9379. doi: 10.1007/s00330-021-08025-2.
13. Son YN, Jin W, Jahng GH, Cha JG, Park YS, Yun SJ *et al.*: Efficacy of double inversion recovery magnetic resonance imaging for the evaluation of the synovium in the femoro-patellar joint without contrast enhancement. Eur Radiol 2018; 28: 459–467. doi: 10.1007/s00330-017-5017-3.
14. Song IH, Althoff CE, Hermann KG, Scheel AK, Knetsch T, Schoenharting M *et al.*: Knee osteoarthritis. Efficacy of a new method of contrast-enhanced musculoskeletal ultrasonography in detection of synovitis in patients with knee osteoarthritis in comparison with magnetic resonance imaging. Ann Rheum Dis 2008; 67: 19–25. doi: 10.1136/ard.2006.067462.
15. Sibbitt WL Jr., Kettwich LG, Band PA, Chavez-Chiang NR, DeLea SL, Haseler LJ *et al.*: Does ultrasound guidance improve the outcomes of arthrocentesis and corticosteroid injection of the knee? Scand J Rheumatol 2012; 41: 66–72. doi: 10.3109/03009742.2011.599071.
16. Gaigneux E, Cormier G, Varin S, Mérot O, Maugars Y, Le Goff B: Ultrasound abnormalities in septic arthritis are associated with functional outcomes. Joint Bone Spine 2017; 84: 599–604. doi: 10.1016/j.jbspin.2017.02.002.
17. Bradley AT, King CA, Cohen-Rosenblum A, Sculco PK, Landy DC: Gout in primary total knee arthroplasty: Prevalent but not independently associated with complications. Knee 2021; 28: 45–50. doi: 10.1016/j.knee.2020.11.007.
18. Upadhyay N, Saifuddin A: The radiographic and MRI features of gout referred as suspected soft tissue sarcoma: a review of the literature and findings from 27 cases. Skeletal Radiol 2015; 44: 467–476. doi: 10.1007/s00256-014-2005-4.
19. Thiele RG: Role of ultrasound and other advanced imaging in the diagnosis and management of gout. Curr Rheumatol Rep 2011; 13: 146–153. doi: 10.1007/s11926-010-0156-4.
20. Girish G, Glazebrook KN, Jacobson JA: Advanced imaging in gout. AJR Am J Roentgenol 2013; 201: 515–525. doi: 10.2214/AJR.13.10776.
21. Filippucci E, Scire CA, Delle Sedie A, Iagnocco A, Riente L, Meenagh G *et al.*: Ultrasound imaging for the rheumatologist. XXV. Sonographic assessment of the

knee in patients with gout and calcium pyrophosphate deposition disease. Clin Exp Rheumatol 2010; 28: 2–5.

22. Yu JS, Chung C, Recht M, Dailiana T, Jurdi R: MR imaging of tophaceous gout. AJR Am J Roentgenol 1997; 168: 523–527. doi: 10.2214/ajr.168.2.9016240.
23. Skovgaard Larsen LP, Rasmussen OS: Diagnosis of acute rupture of the anterior cruciate ligament of the knee by sonography. Eur J Ultrasound 2000; 12: 163–167. doi: 10.1016/s0929-8266(00)00109-9.
24. Kumar S, Kumar A, Kumar S, Kumar P: Functional ultrasonography in diagnosing anterior cruciate ligament injury as compared to magnetic resonance imaging. Indian J Orthop 2018; 52: 638–644. doi: 10.4103/ortho.IJOrtho_28_17.
25. Wu WT, Lee TM, Mezian K, Naňka O, Chang KV, Özçakar L: Ultrasound imaging of the anterior cruciate ligament: a pictorial essay and narrative review. Ultrasound Med Biol 2022; 48: 377–396. doi: 10.1016/j.ultrasmedbio.2021.11.004.
26. Breukers M, Haase D, Konijnenberg S, Klos TVS, Dinant GJ, Ottenheijm RPG: Diagnostic accuracy of dynamic ultrasound imaging in partial and complete anterior cruciate ligament tears: a retrospective study in 247 patients. BMJ Open Sport Exerc Med 2019; 5: e000605. doi: 10.1136/bmjsem-2019-000605.
27. Cho KH, Lee DC, Chhem RK, Kim SD, Bouffard JA, Cardinal E *et al.*: Normal and acutely torn posterior cruciate ligament of the knee at US evaluation: preliminary experience. Radiology 2001; 219: 375–380. doi: 10.1148/radiology.219.2.r01ma22375.
28. Andrews K, Lu A, McKean L, Ebraheim N: Review: Medial collateral ligament injuries. J Orthop 2017; 14: 550–554. doi: 10.1016/j.jor.2017.07.017.
29. De Maeseneer M, Van Roy F, Lenchik L, Barbaix E, De Ridder F, Osteaux M: Three layers of the medial capsular and supporting structures of the knee: MR imaging-anatomic correlation. Radiographics 2000; 20 Spec No: S83–89. doi: 10.1148/radiographics.20.suppl_1.g00oc05s83.
30. Recondo JA, Salvador E, Villanúa JA, Barrera MC, Gervás C, Alústiza JM: Lateral stabilizing structures of the knee: functional anatomy and injuries assessed with MR imaging. Radiographics 2000; 20: S91–S102. doi: 10.1148/radiographics.20.suppl_1.g00oc02s91.
31. Carneiro BC, Araújo FF, Guimarães JB, Chemin RN, Jorge RB, Filho AGO *et al.*: Stener-like lesions in the hand, knee and foot: a review of anatomy, mechanism of injury and imaging evaluation. Clin Imaging 2021; 76: 235–246. doi: 10.1016/j.clinimag.2021.05.001.
32. Gupta N, Taylor RE, Lambert B, Dong D, Phillips P, Jack RA 2nd *et al.*: Shear wave elastography of the ulnar collateral ligament in division IA pitchers across a competitive collegiate season. JSES Int 2023: 7: 703–708. doi: 10.1016/j.jseint.2023.03.014.
33. Taljanovic MS, Gimber LH, Becker GW, Latt LD, Klauser AS, Melville DM *et al.*: Shear-wave elastography: basic physics and musculoskeletal applications. Radiographics 2017; 37: 855–870. doi: 10.1148/rg.2017160116.
34. Wadugodapitiya S, Sakamoto M, Tanaka M, Sakagami Y, Morise Y, Kobayashi K. Assessment of knee collateral ligament stiffness by strain ultrasound elastography. Biomed Mater Eng 2022; 33: 337–349. doi: 10.3233/BME-211282.
35. Meyer P, Reiter A, Akoto R, Steadman J, Pagenstert G, Frosch KH *et al.*: Imaging of the medial collateral ligament of the knee: a systematic review. Arch Orthop Trauma Surg 2022; 142: 3721–3736. doi: 10.1007/s00402-021-04200-8.
36. Watura C, Morgan C, Flaherty D, Gibbons C, Sookur P: Medial collateral ligament injury of the knee: correlations between MRI features and clinical gradings. Skeletal Radiol 2022; 51: 1225–1233. doi: 10.1007/s00256-021-03949-8.
37. Brimmo OA, Senne JA, Crim J: MRI findings of Stener-like lesion of the knee: A case series with surgical correlation. Eur J Radiol 2019; 121: 108709. doi: 10.1016/j.ejrad.2019.108709.
38. Lee JI, Song IS, Jung YB, Kim YG, Wang CH, Yu H *et al.*: Medial collateral ligament injuries of the knee: ultrasonographic findings. J Ultrasound Med 1996; 15: 621–625. doi: 10.7863/jum.1996.15.9.621.
39. Slane LC, Slane JA, Scheys L: The measurement of medial knee gap width using ultrasound. Arch Orthop Trauma Surg 2017; 137: 1121–1128. doi: 10.1007/s00402-017-2740-9.
40. Sekiya JK, Jacobson JA, Wojtys EM: Sonographic imaging of the posterolateral structures of the knee: findings in human cadavers. Arthroscopy 2002; 18: 872–881. doi: 10.1053/jars.2002.32845.
41. Oei EH, Nikken JJ, Verstijnen AC, Ginai AZ, Myriam Hunink MG: MR imaging of the menisci and cruciate ligaments: a systematic review. Radiology 2003; 226: 837–848. doi: 10.1148/radiol.2263011892.
42. Stensby JD, Pringle LC, Crim J: MRI of the meniscus. Clin Sports Med 2021; 40: 641–655. doi: 10.1016/j.csm.2021.05.004.
43. Azzoni R, Cabitza P: Is there a role for sonography in the diagnosis of tears of the knee menisci? J Clin Ultrasound 2002; 30: 472–476. doi: 10.1002/jcu.10106.
44. Guillin R, Marchand AJ, Roux A, Niederberger E, Duvauferrier R: Imaging of snapping phenomena. Br J Radiol 2012; 85: 1343–1353. doi: 10.1259/bjr/52009417.
45. Marchand AJ, Proisy M, Ropars M, Cohen M, Duvauferrier R, Guillin R: Snapping knee: imaging findings with an emphasis on dynamic sonography. AJR Am J Roentgenol 2012; 199: 142–150. doi: 10.2214/AJR.11.7817.
46. Guillin R, Mendoza-Ruiz JJ, Moser T, Ropars M, Duvauferrier R, Cardinal E: Snapping biceps femoris tendon: a dynamic real-time sonographic evaluation. J Clin Ultrasound 2010; 38: 435–437. doi: 10.1002/jcu.20728.
47. Kennedy MI, DePhillipo NN, Chahla J, Armstrong C, Ziegler CG, Buckley PS *et al.*: Surgical repair of dynamic snapping biceps femoris tendon. Arthrosc Tech 2018; 7: e1129–e1133. doi: 10.1016/j.eats.2018.07.010.
48. Koh YG, Kim SJ, Chun YM, Kim YC, Park YS: Arthroscopic treatment of patellofemoral soft tissue impingement after posterior stabilized total knee arthroplasty. Knee 2008; 15: 36–39. doi: 10.1016/j.knee.2007.08.009.
49. Okamoto T, Futani H, Atsui K, Fukunishi S, Koezuka A, Maruo S: Sonographic appearance of fibrous nodules in patellar clunk syndrome: a case report. J Orthop Sci 2002; 7: 590–593. doi: 10.1007/s007760200106.
50. Geannette C, Miller T, Saboeiro G, Parks M: Sonographic evaluation of patellar clunk syndrome following total knee arthroplasty. J Clin Ultrasound 2017; 45: 105–107. doi: 10.1002/jcu.22389.
51. Falkowski AL, Jacobson JA, Hirschmann MT, Kalia V: MR imaging of the quadriceps femoris tendon: distal tear characterization and clinical significance of rupture types. Eur Radiol 2021; 31: 7674–7683. doi: 10.1007/s00330-021-07912-y.
52. Warden SJ, Kiss ZS, Malara FA, Ooi AB, Cook JL, Crossley KM: Comparative accuracy of magnetic resonance imaging and ultrasonography in confirming clinically diagnosed patellar tendinopathy. Am J Sports Med 2007; 35: 427–436. doi: 10.1177/0363546506294858.
53. Breda SJ, van der Vlist A, de Vos RJ, Krestin GP, Oei EHG: The association between patellar tendon stiffness measured with shear-wave elastography and patellar tendinopathy – a case-control study. Eur Radiol 2020; 30: 5942–5951. doi: 10.1007/s00330-020-06952-0.
54. Gulledge CM, Baumer TG, Juliano L, Sweeney M, McGinnis M, Sherwood A *et al.*: Shear wave elastography of the healing human patellar tendon following ACL reconstruction. Knee 2019; 26: 347–354. doi: 10.1016/j.knee.2018.12.006.
55. Akkaya S, Akkaya N, Agladioglu K, Gungor HR, Ok N, Ozcakar L: Real-time elastography of patellar tendon in patients with auto-graft bone-tendon-bone anterior cruciate ligament reconstruction. Arch Orthop Trauma Surg 2016; 136: 837–842. doi: 10.1007/s00402-016-2459-z.
56. Ito N, Sigurðsson HB, Pohlig RT, Cortes DH, Gravare Silbernagel K, Sprague AL: Reliability of continuous shear wave elastography in the pathological patellar tendon. J Ultrasound Med 2023; 42: 1047–1055. doi: 10.1002/jum.16115.
57. Telischak NA, Wu JS, Eisenberg RL: Cysts and cystic-appearing lesions of the knee: A pictorial essay. Indian J Radiol Imaging 2014; 24: 182–191. doi: 10.4103/0971-3026.134413.